

DOPING DEPENDENCE OF CORRELATION EFFECTS IN $K_{1-x}Fe_{2-y}Se_2$ SUPERCONDUCTORS: LDA'+DMFT INVESTIGATION

I. A. Nekrasov^a, N. S. Pavlov^{a}, M. V. Sadovskii^{a,b}*

^a*Institute for Electrophysics, Russian Academy of Sciences, Ural Branch
620016, Ekaterinburg, Russia*

^b*Institute for Metal Physics, Russian Academy of Sciences, Ural Branch
620990, Ekaterinburg, Russia*

Received April 23, 2013

We present a detailed LDA'+DMFT investigation of the doping dependence of correlation effects in the novel $K_{1-x}Fe_{2-y}Se_2$ superconductor. Calculations are performed at four different hole doping levels, starting from a hypothetical stoichiometric composition with the total number of electrons equal to 29 per unit cell through 28 and 27.2 electrons toward the case of 26.52, which corresponds to the chemical composition $K_{0.76}Fe_{1.72}Se_2$ studied in recent ARPES experiments. In the general case, the increase in hole doping leads to quasiparticle bands in a wide energy window ± 2 eV around the Fermi level becoming more broadened by lifetime effects, while correlation-induced compression of Fe-3d LDA' bandwidths stays almost the same, of the order of 1.3 for all hole concentrations. However, close to the Fermi level, the situation is more complicated. In the energy interval from -1.0 eV to 0.4 eV, the bare Fe-3d LDA' bands are compressed by significantly larger renormalization factors up to 5 with increased hole doping, while the value of Coulomb interaction remains the same. This fact manifests the increase in correlation effects with hole doping in the $K_{1-x}Fe_{2-y}Se_2$ system. Moreover, in contrast to typical pnictides, $K_{1-x}Fe_{2-y}Se_2$ does not have well-defined quasiparticle bands on the Fermi levels, but has a "pseudogap"-like dark region instead. We also find that with the growth of hole doping Fe-3d orbitals of various symmetries are affected by correlations differently in different parts of the Brillouin zone. To illustrate this, we determine the quasiparticle mass renormalization factors and energy shifts that transform the bare Fe-3d LDA' bands of various symmetries into LDA'+DMFT quasiparticle bands. These renormalization factors effectively mimic more complicated energy-dependent self-energy effects and can be used to analyze the available ARPES data.

DOI: 10.7868/S0044451013110163

1. INTRODUCTION

The discovery of iron based high-temperature superconductors [1] stimulated quite intensive research work [2–6]. Recently, another class of high- T_c superconductors isostructural to the 122 family of iron pnictides was discovered, iron chalcogenides $K_xFe_2Se_2$ [7], $Cs_xFe_2Se_2$ [8] and $(Tl,K)Fe_xSe_2$ [9]. The values of the superconducting critical temperatures T_c are comparable for both families of pnictides and chalcogenides and are about 30–50 K [10–13]. Further interest in these chalcogenides was stimulated by the experimental observation of rather nontrivial antiferromagnetic orde-

ring with a very high Neel temperature about 550 K and the ordering of Fe vacancies in the same range of temperatures in $K_{0.8}Fe_{1.6}Se_2$ (the so-called 245 phase) [14]. Despite of intensive experimental work, there is still no consensus on the composition of the phase responsible for the high- T_c superconductivity in these systems. The most common point of view is that KFe_2Se_2 (the 122 phase) is the parent compound for superconductivity, while the 245 phase is insulating [6, 15, 16]. Some other phases in this system were also reported [17]. Below, we concentrate on electronic structure calculations for the parent 122 phase with different levels of hole doping.

Crystallographically, pnictides AFe_2As_2 and chalcogenides $Fe(Se,Te)$ and AFe_2Se_2 are quite similar, with the main structural motif determined by layers of

*E-mail: pavlov@iep.uran.ru

Fe(As,Se)₄ tetrahedra. Recently reported theoretical electronic band structures of Fe(Se,Te) [18] and AFe₂As₂ [19–21] are found to be nearly identical to each other, especially for the bands crossing the Fermi level. AFe₂As₂ and AFe₂Se₂ compounds are simply isostructural. However, the LDA (local density approximation) electronic structure of AFe₂Se₂ differs quite remarkably from that of AFe₂As₂, as was directly shown in Refs. [15, 22, 23].

From the very beginning of studies of iron-based superconductors, it was recognized that the account of electronic correlations on Fe sites is rather essential for the correct description of the physics of pnictide materials [24–27]. For this, the LDA+DMFT hybrid computational scheme [28] was used. The main conclusion was that correlations lead to simple narrowing (compression) of the LDA bandwidth by a factor ranging from 2 or 3. This observation agrees rather well with the variety of angular-resolved photoemission spectroscopy (ARPES) data on AFe₂As₂ compounds [6]. Fermi surface maps obtained from ARPES experiments for AFe₂As₂ are quite similar to those obtained from simple LDA calculations: there are two or three hole cylinders around the Γ point in the Brillouin zone and two electron Fermi surface sheets around the (π, π) point.

Until recently, only a few LDA+DMFT papers were devoted to Fe chalcogenides [29, 30]. We recently investigated the electronic structure of hole-doped iron chalcogenide K_{0.76}Fe_{1.72}Se₂ in the normal phase [31], inspired by available ARPES data for this system [34], especially those obtained in Ref. [35], using both the standard LDA+DMFT and the novel LDA'+DMFT computational approaches [32, 33]. The results of our calculations agree rather well with the general picture of ARPES obtained in Ref. [35], with the LDA'+DMFT results showing a slightly better agreement. We showed that this iron chalcogenide is actually more strongly correlated in the sense of the bandwidth renormalization (energy scale compression by a factor of about 5 in the energy interval ± 1.5 eV around the Fermi level) than the typical iron pnictides (with a compression factor of about 2 or 3 [6]), although the Coulomb interaction strength is almost the same in both families. Moreover, the K_{0.76}Fe_{1.72}Se₂ system demonstrates the absence of well-defined quasiparticle bands on the Fermi level, in contrast to pnictides.

In this paper, we continue our LDA'+DMFT study of the system. We investigate the evolution of correlation effects upon hole doping by performing LDA'+DMFT calculations at four doping levels: the hypothetical stoichiometric composition with 29 valence

electrons per unit cell, through intermediate values of valence electrons 28 and 27.2 down to the experimentally obtained composition K_{0.76}Fe_{1.72}Se₂ with 26.52 electrons per unit cell. We demonstrate in what follows that the actual doping dependence of correlation effects on the electronic structure in iron chalcogenides is apparently more complicated than in iron pnictides and does not reduce to the simple picture of universal bandwidth renormalization (compression).

This paper is organized as follows. In Sec. 2, we discuss the crystallographic structure and methodological and computational details of LDA'+DMFT. A comparative study of LDA' bands and LDA'+DMFT spectral function maps within wide and narrow energy intervals around the Fermi level, together with orbitally resolved densities of states, is presented in Sec. 3. We summarise our results in Sec. 4.

2. COMPUTATIONAL DETAILS

The K_xFe₂Se₂ system is isostructural to Ba122 pnictide (see Ref. [19] for the last one) with the ideal body-centered tetragonal space group I4/mmm. In K_xFe₂Se₂, $a = 3.9136$ Å and $c = 14.0367$ Å with K ions occupying $2a$, Fe ions $4d$ and Se ions $4e$ positions with $z_{\text{Se}} = 0.3539$ [7]. This crystal structure was used in band structure calculations for K_{0.76}Fe_{1.72}Se₂ within the linearized method of muffin-tin orbitals (LMTO) [36] using default settings [23].

To take local Coulomb correlations into account, we here use the LDA'+DMFT [32, 33] approach, which is a modification of the well-known LDA+DMFT method [28]. The LDA+DMFT Hamiltonian is usually written as

$$\hat{H} = \hat{H}^{LDA} + \hat{H}^{Hub} - \hat{H}^{DC}. \quad (1)$$

The general problem with LDA+DMFT is that some portion of local electron–electron interaction for presumed correlated d shells is already included in the standard LDA (\hat{H}^{LDA}). To avoid its double counting due to the Hubbard interaction \hat{H}^{Hub} , we have to subtract the so-called double-counting correction term \hat{H}^{DC} from \hat{H}^{LDA} . (Explicit expressions for \hat{H}^{LDA} and \hat{H}^{Hub} can be found in [33].) The LDA'+DMFT approach is the new attempt to solve the double-counting problem, which is due to the absence of a universal expression for \hat{H}^{DC} , because there is no explicit microscopic (or diagrammatic) link between the model (Hubbard-like) Hamiltonian approach and the standard LDA.

In brief, the main idea of LDA'+DMFT is to explicitly exclude the contribution of the presumably

strongly correlated d shells from the charge density at the initial step of LDA calculations. Then, this redefined charge density (for some chosen orbital basis $\varphi_i(\mathbf{r})$)

$$\rho'(\mathbf{r}) = \sum_{i \neq i_d} |\varphi_i(\mathbf{r})|^2 \quad (2)$$

is used to calculate the local exchange-correlation energy E_{xc}^{LDA} in LDA and perform self-consistent LDA band structure calculations for correlated bands at the LDA stage of LDA+DMFT. The local d - d electron correlations are subsequently taken into account within DMFT. All states not counted as strongly correlated are then treated with the full power of DFT/LDA and the full ρ in E_{xc}^{LDA} .

Once this LDA' calculations with the redefined charge density were done, just the Hartree contribution to the interaction of correlated states is left at the LDA stage; which can be written in the fully localized limit form (FLL), which is the most consistent definition of the double-counting term here (other forms can be also used [33]):

$$\hat{H}_{FLL}^{DC} = \frac{1}{2} U n_d (n_d - 1) - \frac{1}{2} J \sum_{\sigma} n_{d\sigma} (n_{d\sigma} - 1), \quad (3)$$

where $n_{d\sigma} = \sum_m n_{i_d m \sigma} = \sum_m \langle \hat{n}_{i_d m \sigma} \rangle$ is the total number of electrons on strongly interacting orbitals and the number of electrons per spin, $n_d = \sum_{\sigma} n_{d\sigma}$.

The effective five-orbital impurity problem for $K_{1-x}Fe_{2-y}Se_2$ within DMFT was solved by the Hirsh-Fye quantum Monte Carlo algorithm [37] at the temperature 280 K. LDA'+DMFT densities of states and spectral functions were obtained as discussed in Ref. [32]. Coulomb parameters were respectively taken to be $U = 3.75$ eV and $J = 0.6$ eV [35], which are very close to calculated ones [38]. To define the DMFT lattice problem, we used the full LDA Hamiltonian (without downfolding or projecting), which includes all Fe- $3d$, Se- $4p$, and K- $4s$ states.

3. RESULTS AND DISCUSSION

In Fig. 1, we compare the LDA'+DMFT calculated spectral function maps in the wide energy window ± 2 eV along high-symmetry directions in the first Brillouin zone and the renormalized LDA' bands (grey lines) for $K_{1-x}Fe_{2-y}Se_2$ at different hole doping levels n_e . The renormalization (bandwidth compression) factor of LDA' bands here is only 1.3, and hence the bandwidth renormalization due to correlations is rather weak. The lower panel in Fig. 1 shows LDA'+DMFT

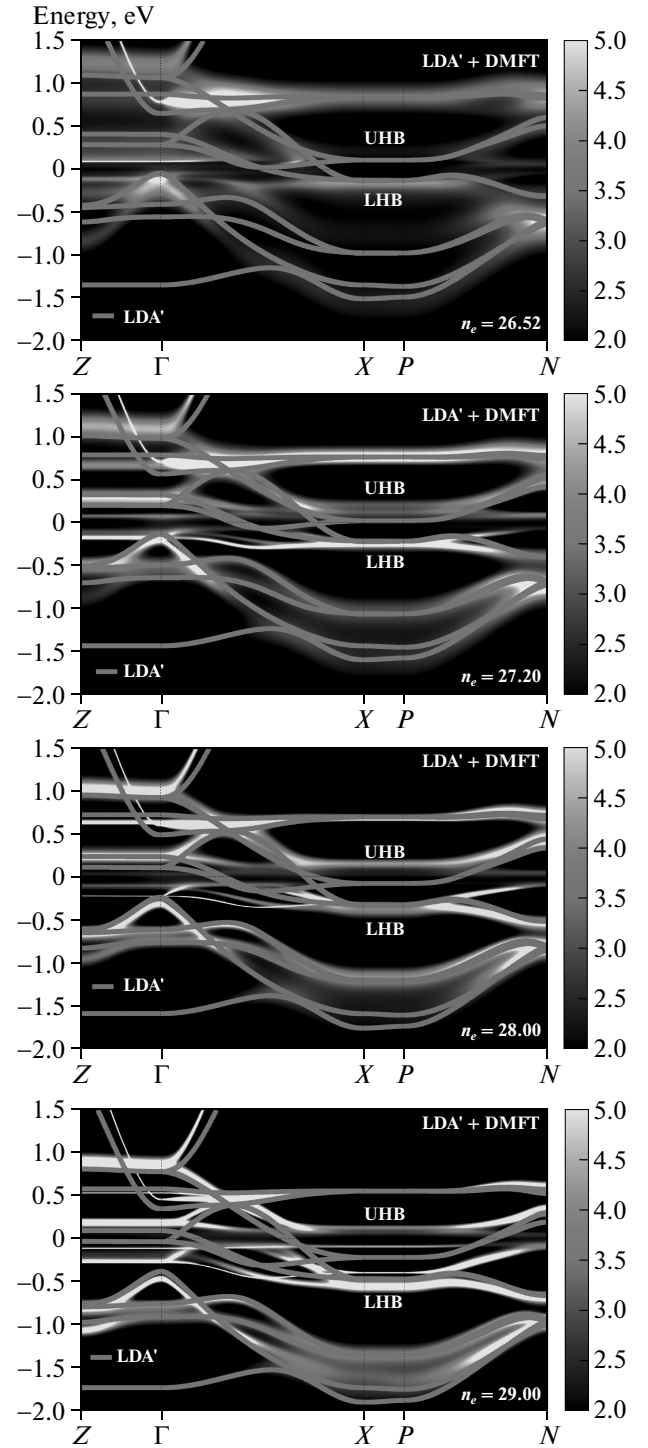


Fig. 1. Comparison of LDA'+DMFT calculated spectral function maps with LDA' bands renormalized by the compression factor 1.3 (grey lines) for $K_{1-x}Fe_{2-y}Se_2$ for different hole doping levels: $n_e = 29, 28, 27.2, 26.52$ (from bottom up) along the high-symmetry direction of the first Brillouin zone. The Fermi level is zero

data for the stoichiometric KFe_2Se_2 compound with the total number of valence electrons $n_e = 29$. For this composition, all quasiparticle bands are rather well defined for this wide energy range around the Fermi level. In the hole-doped cases with $n_e = 28, 27.2, 26.52$ (2nd, 3rd and 4th panels from bottom up), we see that Fe-3d bands obtained from LDA'+DMFT become less pronounced with hole doping. The overall rigid shift of LDA' bands from the stoichiometric case down to the most hole doped one is about 0.3 eV.

In Fig. 2, we show LDA'+DMFT spectral function maps in the vicinity (-0.5 – 0.2 eV) of the Fermi level with the dominant orbital character of quasiparticle bands denoted explicitly by black squares for xz and yz , black circles for xy , white circles for $3z^2 - r^2$, and white squares for $x^2 - y^2$. We can see that the orbital characters and forms of quasiparticle bands in this energy interval (-0.1 – 0.1 eV) change with the increase in hole doping, although characters of quasiparticle bands located outside this region remain the same. The main orbital character of bands crossing the Fermi level is xz , yz , and xy . From Fig. 2, we can also conclude that sufficiently close to the Fermi level (for all hole dopings), there are uniformly no well-defined quasiparticle bands (although some low-intensity maxima of the spectral density can still be seen). This implies that for all hole dopings, $\text{K}_{1-x}\text{Fe}_{2-y}\text{Se}_2$ is more correlated than the 122 pnictide system.

This “pseudogap”-like behaviour can be explicitly observed in Fig. 3 for all Fe-3d orbitals, where orbitally resolved bare LDA' and LDA'+DMFT densities of states (DOS) for all four hole doping levels are presented. Inspecting these DOSes shows that the effects become stronger upon hole doping correlation. This fact manifests itself in a different way for orbitals of various symmetry. First of all, for all Fe-3d orbitals, we observe a narrowing of DOSs. For $3z^2 - r^2$ (the third panel from top) and $x^2 - y^2$ (the upper panel), this narrowing is most evident at ± 1 eV and ± 0.5 eV. For xz , yz (the second panel from top), and xy (the bottom panel), the increase in narrowing with doping is mostly concentrated in the energy interval ± 0.4 eV.

To obtain a deeper insight into the LDA'+DMFT self-energy effects on bare LDA' bands, we have determined energy scale renormalizations and energy shifts for a variety of separate dispersions of the bare LDA' band structure depicted in Fig. 4, which rather accurately fit bare bands to those plotted in Fig. 2. Also in Fig. 4 we show the standard LDA bands (dashed lines), just to emphasize that LDA' dispersions are quite close to the LDA ones (also see Refs. [31–33]). The obtained energy scale renormalization (bandwidth compression)

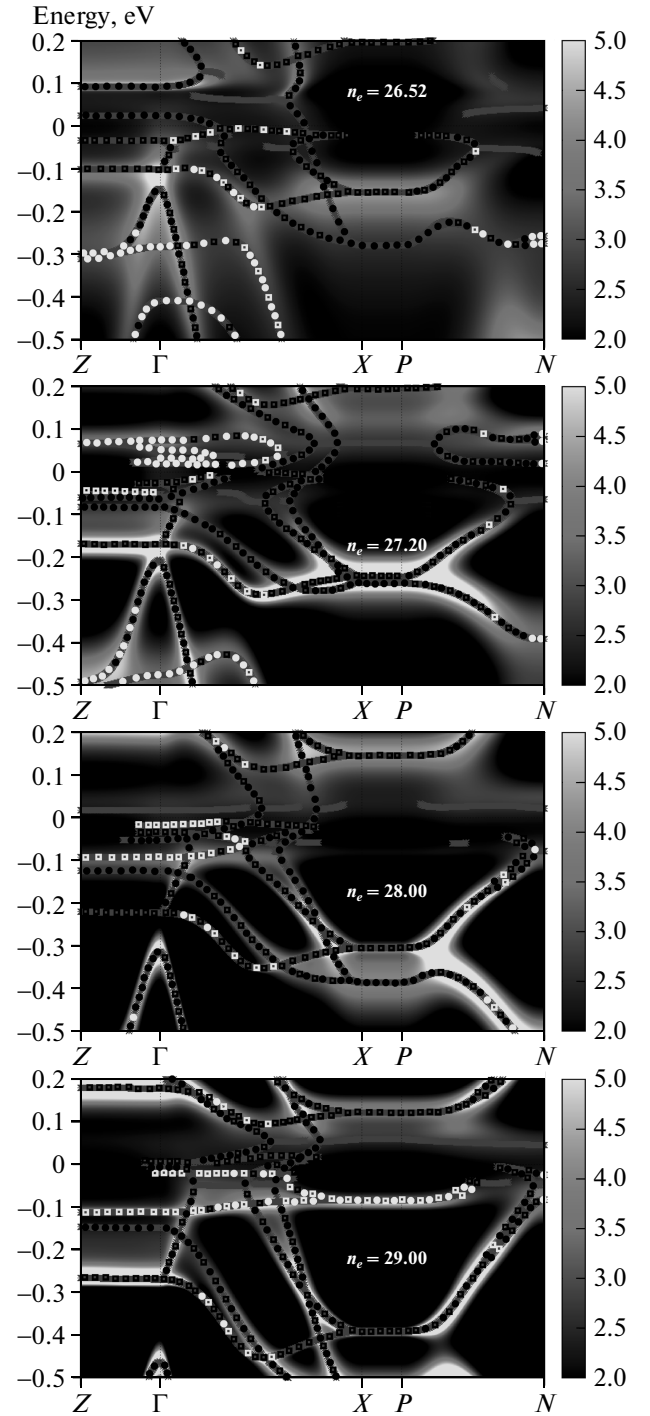


Fig. 2. LDA'+DMFT spectral density maps along high-symmetry directions of the first Brillouin zone. Intensity maxima are shown by stars. The dominant orbital character of quasiparticle bands is marked as follows: black squares, xz , yz ; black circles, xy ; white circles, $3z^2 - r^2$; white squares, $x^2 - y^2$. The Fermi level is zero

Table. Quasiparticle energy scale renormalization factors and the corresponding energy shifts (in eV, in round brackets) for different bare Fe-3d LDA' orbitals for all hole doping levels n_e in the LDA' scale energy interval from -1.0 eV to 0.4 eV

Orbital character	$n_e = 26.52$	$n_e = 27.20$	$n_e = 28.00$	$n_e = 29.00$
xy	1.5 (-0.23)	3.9 (-0.73)	2.65 (-0.61)	1.7 (-0.35)
xz, yz (1)	4.2 (-0.78)	3.0 (-0.75)	2.6 (-0.69)	1.7 (-0.38)
xz, yz (2)	2.3 (-0.48)	2.5 (-0.60)	2.6 (-0.69)	1.7 (-0.38)
xy, xz, yz	1.2 (-0.10)	1.3 (-0.10)	1.3 (-0.10)	1.4 (-0.17)
$3z^2 - r^2$	4.7 (-0.85)	2.0 (-0.30)	1.3 (-0.03)	1.25 (0.0)

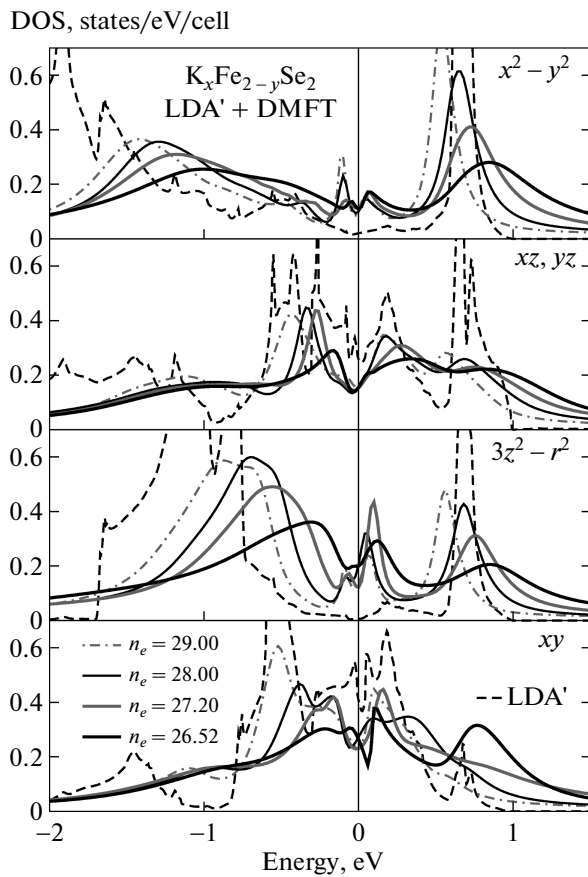


Fig. 3. Comparison of LDA' (dashed black line) and LDA'+DMFT density of states (DOS) for $K_{1-x}Fe_{2-y}Se_2$ for different dopings n_e . The thick black line corresponds to $n_e = 26.52$, the thick grey line, to $n_e = 27.20$, the thin black line, to $n_e = 28.00$, the grey dot-dashed line, to $n_e = 29.00$. The Fermi level is zero

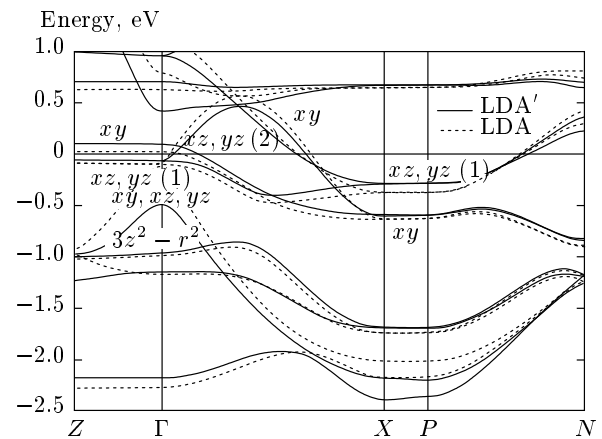


Fig. 4. Bare LDA' (full line) and LDA (dashed line) band dispersions for the stoichiometric KFe_2Se_2 system with the orbital characters explicitly shown. The numbers in brackets after the orbital symmetry symbols enumerate the corresponding parts of the bands in the first Brillouin zone (see Table)

factors and energy shifts (shown in brackets) are collected in Table for all hole doping levels. These results show a more complicated picture of bare LDA' dispersion transformations than the one obtained in Ref. [31], where we proposed that all Fe-3d band dispersions for the $K_{0.76}Fe_{1.72}Se_2$ should be compressed by a factor of 5 to obtain reasonable agreement with experiment. In contrast to our previous work in [31], we here fit LDA' bare bands exactly to maxima positions of the spectral function (see stars in Fig. 2). We thus obtain a more detailed picture, which in general agrees with our early conclusions in Ref. [31].

Here, we actually see that different parts of bands in the first Brillouin zone acquire different (bandwidth or mass) renormalization factors, which change with

doping. For example, the xy , xz , yz band (see Fig. 4) has almost no doping dependence at all (see Table). The renormalization for the part of xz, yz band (2) only slightly depends on doping. However, xz, yz band (1) becomes monotonically more correlated (the renormalization factor increases to 4.2) as hole doping increases. The correlation renormalization of the xy orbital demonstrates nonmonotonic behavior and is more pronounced for intermediate dopings. The renormalization factor of the $3z^2 - r^2$ band near the Γ point abruptly increases to 4.7 at $n_e = 26.52$. We note that all four doping levels were treated with the same Coulomb interaction parameters. Despite this fact, several orbitals of $K_{1-x}Fe_{2-y}Se_2$ become more correlated (narrowed) upon doping. This phenomenon is apparently related to the change of the correlated orbital occupancy. The data collected in Table might be helpful in interpreting ARPES spectra in simple terms of renormalized bare LDA band dispersions.

4. CONCLUSIONS

In this paper, we have performed a detailed LDA'+DMFT study of correlation effects in the $K_{1-x}Fe_{2-y}Se_2$ system at four hole doping levels: from the hypothetical stoichiometric composition with 29 valence electrons per unit cell, through intermediate values of valence electrons 28 and 27.2, toward the composition $K_{0.76}Fe_{1.72}Se_2$ with 26.52 electrons per unit cell, for which there are available ARPES data on electronic dispersions [35].

Within DMFT, correlation effects are concentrated in the self-energy, which provides two types of modifications of the bare spectra at each energy: broadening (lifetime effects) by the imaginary part of self-energy and the energy shift due to its real part. We have shown that in a rather wide energy window ± 2 eV (in terms of the LDA energy scale) for all dopings, the lifetime effects are relatively weak and the renormalization (compression) of quasiparticle bandwidths remains nearly the same and of the order of 1.3. But near the Fermi level, self-energy effects become more pronounced and complicated. In particular, the renormalization (bandwidth compression) factor increases from 1.3 for the stoichiometric composition to nearly 5 for $K_{0.76}Fe_{1.72}Se_2$ (for xz, yz , and $3z^2 - r^2$ bands). Although all calculations were done with the same value of the Coulomb (Hubbard) interaction, this increase of renormalization upon doping tells us that correlations also increase with doping. Also following the recent tendency of experimental ARPES papers,

where energy shifts and renormalization factors are determined separately for different bare LDA bands [6, 34] to fit ARPES data, we have provided quasiparticle mass renormalizations and energy shifts, which rather accurately transform bare Fe-3d LDA' bands of various symmetries into LDA'+DMFT quasiparticle bands in different regions of the first Brillouin zone. In fact, the detailed picture of band renormalizations close to the Fermi level in $K_{1-x}Fe_{2-y}Se_2$ is quite complicated. For example, the xy, xz , and yz bands near the Γ point and the $xz, yz(2)$ bands in the middle of Γ -X and P-N directions almost do not feel doping changes. By contrast, the $xz, yz(1)$ bands in all directions and the $3z^2 - r^2$ band near the Γ point become monotonically more correlated (renormalized) as doping increases. Finally, correlation renormalization of the xy band demonstrates nonmonotonic behavior with doping, becoming more correlated for intermediate dopings. However, the general conclusion in Ref. [23] remains valid: the $K_{1-x}Fe_{2-y}Se_2$ systems demonstrate more pronounced correlation effects in contrast to 122 iron pnictides. This is clearly reflected in the absence of well-defined quasiparticle bands in the vicinity of the Fermi level, which demonstrates a kind of "pseudogap" behavior (the "dark" region around the Fermi level in Fig. 2). An interesting problem for the future studies is possible manifestation of these effects in optical conductivity, as well as their role in the formation of the superconducting state.

We thank A. I. Poteryaev for providing us with the QMC code and many helpful discussions. This work is partly supported by the RFBR grant 11-02-00147 and was performed in the framework of programs of fundamental research of the Russian Academy of Sciences (RAS) "Quantum mesoscopic and disordered structures" (12-II-2-1002) and of the Physics Division of RAS "Strongly correlated electrons in solids and structures" (012-T-2-1001). NSP acknowledges the support of the Dynasty Foundation and the International Center of Fundamental Physics in Moscow. DMFT (QMC) calculations were performed on the supercomputer "Uran" at the Institute of Mathematics and Mechanics, UB RAS.

REFERENCES

1. Y. Kamihara, T. Watanabe, M. Hirano, and H. Hosono, *J. Amer. Chem. Soc.* **130**, 3296 (2008).
2. M. V. Sadovskii, *Uspekhi Fiz. Nauk* **178**, 1243 (2008); arXiv:0812.0302.

3. K. Ishida, Y. Nakai, and H. Hosono, *J. Phys. Soc. Jpn.* **78**, 062001 (2009).
4. Y. Mizuguchi and Y. Takano, *J. Phys. Soc. Jpn.* **79**, 102001 (2010).
5. P. J. Hirschfeld, M. M. Korshunov, and I. I. Mazin, *Rep. Progr. Phys.* **74**, 124508 (2011)
6. A. A. Kordyuk, *Fizika Nizkikh Temperatur* **38**, 1119 (2012); arXiv:1209.0140.
7. J. Guo, S. Jin, G. Wang et al., *Phys. Rev. B* **82**, 180520(R) (2010).
8. A. Krzton-Maziopa, Z. Siermadini, E. Pomjakushina et al., *J. Phys.: Condens. Matter* **23**, 052203 (2011).
9. M. Fang, H. Wang, C. Dong et al., *Phys. Rev. B* **84**, 224506 (2011).
10. M. Rotter, M. Tegel, and D. Johrendt, *Phys. Rev. Lett.* **101**, 107006 (2008).
11. G.F. Chen, Z. Li, G. Li et al., *Chin. Phys. Lett.* **25**, 3403 (2008); arXiv:0806.1209.
12. K. Sasmal, B. Lv, B. Lorenz et al., *Phys. Rev. Lett.* **101**, 107007 (2008).
13. N. Ni, S. L. Bud'ko, A. Kreyssig et al., *Phys. Rev. B* **78**, 014507 (2008).
14. W. Bao, Q. Huang, G. F. Chen et al., *Chin. Phys. Lett.* **28**, 086104 (2011); arXiv:1102.0830.
15. M. V. Sadovskii, E. Z. Kuchinskii, and I. A. Nekrasov, *J. Magn. Magn. Mater.* **324**, 3481 (2012); arXiv:1106.3707.
16. Hai-Hu Wen, *Rep. Progr. Phys.* **75**, 112501 (2012).
17. W. Li, H. Ding, Z. Li et al., *Phys. Rev. Lett.* **109**, 057003 (2012).
18. A. Subedi, L. Zhang, D. J. Singh, and M. H. Du, *Phys. Rev. B* **78**, 134514 (2008).
19. I. A. Nekrasov, Z. V. Pchelkina, and M. V. Sadovskii, *Pis'ma Zh. Eksp. Teor. Fiz.* **88**, 155 (2008); arXiv:0806.2630.
20. I. R. Shein and A. L. Ivanovskii, *Pis'ma Zh. Eksp. Teor. Fiz.* **88**, 115 (2008); arXiv:0806.0750.
21. C. Krellner, N. Caroca-Canales, A. Jesche et al., *Phys. Rev. B* **78**, 100504(R) (2008).
22. I. R. Shein and A. L. Ivanovskii, *Phys. Lett. A* **375**, 1028 (2011); arXiv:1012.5164v1.
23. I. A. Nekrasov and M. V. Sadovskii, *Pis'ma Zh. Eksp. Teor. Fiz.* **93**, 182 (2011); arXiv:1101.0051.
24. K. Haule, J. H. Shim, and G. Kotliar, *Phys. Rev. Lett.* **100**, 226402 (2008).
25. L. Craco, M. S. Laad, S. Leoni, and H. Rosner, *Phys. Rev. B* **78**, 134511 (2008).
26. A. O. Shorikov, M. A. Korotin, S. V. Streltsov, D. M. Korotin, and V. I. Anisimov, *Zh. Eksp. Teor. Fiz.* **135**, 134 (2009); arXiv:0804.3283.
27. S. L. Skornyakov, A. V. Efremov, N. A. Skorikov et al., *Phys. Rev. B* **80**, 092501 (2009).
28. K. Held, I. A. Nekrasov, N. Blümer, V. I. Anisimov, and D. Vollhardt, *Int. J. Mod. Phys. B* **15**, 2611 (2001); G. Kotliar, S. Y. Savrasov, K. Haule et al., *Rev. Mod. Phys.* **78**, 865 (2006).
29. L. Craco, M. S. Laad, and S. Leoni, arXiv:0910.3828; L. Craco and M. S. Laad, arXiv:1001.3273.
30. L. Craco, M. S. Laad, and S. Leoni, arXiv:1109.0116.
31. I. A. Nekrasov, N. S. Pavlov, and M. V. Sadovskii, *Pis'ma Zh. Eksp. Teor. Fiz.* **97**, 18 (2013); arXiv:1211.3499
32. I. A. Nekrasov, N. S. Pavlov, and M. V. Sadovskii, *Pis'ma v ZhETF* **95**, 659 (2012); arXiv:1204.2361.
33. I. A. Nekrasov, N. S. Pavlov, and M. V. Sadovskii, *Zh. Eksp. Teor. Fiz.* **143**, 713 (2013); arXiv:1208.4732.
34. Y. Zhang, L. X. Yang, M. Xu et al., *Nature Mater.* **10**, 273 (2011), arXiv:1012.5980; X.-P. Wang, T. Qian, P. Richard et al., *Europhys. Lett.* **93**, 57001 (2011), arXiv:1101.4923; D. Mou, Sh. Liu, X. Jia et al., *Phys. Rev. Lett.* **106**, 107001 (2011); L. Zhao, D. Mou, Sh. Liu et al., *Phys. Rev. B* **83**, 140508(R) (2011).
35. M. Yi, D. Lu, R. Yu et al., *Phys. Rev. Lett.* **110**, 067003 (2013); arXiv:1208.5192.
36. O. K. Andersen, *Phys. Rev. B* **12**, 3060 (1975); O. Gunnarsson, O. Jepsen, and O. K. Andersen. *Phys. Rev. B* **27**, 7144 (1983); O. K. Andersen and O. Jepsen. *Phys. Rev. Lett.* **53**, 2571 (1984).
37. J. E. Hirsch and R. M. Fye, *Phys. Rev. Lett.* **56**, 2521 (1986).
38. V. I. Anisimov, Dm. M. Korotin, M. A. Korotin et al., *J. Phys. Cond. Matt.* **21**, 075602 (2009).